Experimental and Theoretical results in Nondestructive Evaluation using HTS-SQUIDs

Adele Ruosi and Massimo Valentino

Istituto Nazionale per la Fisica della Materia, Dip. Scienze Fisiche, Universita' di Napoli, Italy

Abstract. A summary of the experimental and theoretical results carried on at the University of Naples in the framework of the INFM project titled "Eddy-current nondestructive evaluation by superconductive devices" is presented. We emphasize the work that has been done in detecting artificial damages on planar structures of materials interesting for the aeronautic industry such as Al alloy and reinforced carbon fiber polymer. Comparison between the performance of traditional e.m. probes working at room temperature, such as flux-gates and induction coils and the innovative magnetometer based on high critical temperature superconductors showed the overall superiority of the superconductive probe in these niches of applications. Two numerical modelling one based on the finite element method and the other on the volume integral formulation have been successfully developed to simulate the response of the new system to different type of flaws in Al-alloy planar structures. The second one, in the localized non-linear approximation, has been used to solve the inverse e.m. problem which enables to retrieve the parameters of the defects from the experimental data.

In addition novel tools developed to monitor niobium chemistry during fabrication of nuclear resonant cavities and to test current distributions inside power modules used in motor for railways transportation both based on the traditional flux-gate magnetometry are discussed.

I. Introduction

The combination of high sensitivity, even in unshielded environment, high spatial resolution and flat frequency response up to 1 MHz offered by superconducting quantum interference device (SQUID) magnetometers, make them a powerful probe for eddy current nondestructive materials evaluation and inspection [1-4]. Due to the above-mentioned characteristics, SQUIDs are well suited both in the detection of deeply embedded defects into conductive structure and in the inspection of surface defects through surface coatings several millimetres thick. Indeed, traditional eddy current measuring devices need a rather high operating frequency (typically, a few hundred kHz) which strongly limits the skin depth into the conductive material.

The need to operate the SQUID at the very low cryogenic temperature of liquid helium limits its use in many applications. The advent of high critical temperature superconductors (HTS) working at liquid nitrogen temperature and the development of HTS-SQUIDs has renewed the interest for non-destructive evaluation (NDE) based on superconducting sensors [for a review see ref.5].

The INFM project titled “Eddy-current non-destructive evaluation by superconductive devices" supported by the European Community (FESR funds) enabled to exploit the expertise of our group in this emerging field [6].

A 3-channels NDE system based on HTS-SQUIDs, mainly devoted to noninvasive analysis of electrically conductive materials in fields of applications such as aircraft industry and airplanes maintenance, has been designed and set–up. In addition we equipped our laboratory with different traditional e.m. probes. Our research tackled different aspects on NDE. A round robin test for the detection of flaws which result from the machining process or aging of planar stratified structures such as those commonly encountered in the aircraft industry has been carried out by different eddy-current probes. In particular, the performance of an induction coil, a flux-gate and a HTS-SQUID-based magnetometer has been investigated on the basis of comparative experiments on single-layered and multi-layered Al-alloy samples with artificial defects. The overall superiority of the HTS-SQUID-based magnetometer with respect to these more traditional devices in the identification of deep artificial defects such as holes, slots and cracks has been demonstrated in these cases.

To evaluate the accuracy and reliability of the measuring system, two different three-dimensional numerical models of the eddy-current perturbation (electromagnetic direct problem) of electrically conductive plates affected by flaws, were implemented. The formulation based on a finite element method was tackled in collaboration with the Centro Italiano Ricerche Aerospaziali CIRA, Capua, Italy. A less computationally demanding model cast in a vector wavefield integral equation framework was developed in collaboration with DRÉ-LSS, CNRS-SUPÉLEC, Gif-sur-Yvette Cedex, France. In both cases the numerical solutions correctly predicts the shape and amplitude of the complicated magnetic field response, which results from the shape of the defects, the geometry of the inducing coil and the characteristics of the SQUID gradiometer. Moreover the inversion problem was tackled and measured signals have been processed to retrieve pertinent features of the defects.

Our investigation has also been extended to materials of higher complexity, used in aircraft industry, e.g. quasi-isotropic N-ply reinforced carbon fiber polymer panels. Also in this application, interesting for the in-service airplanes maintenance, the better performance of the SQUID in

detecting areas damaged by low-velocity impacts as compared to other traditional probes was demonstrated.

In emerging fields of application of the magnetometry and/or where the high performance of SQUID are not required we first demonstrate the feasibility of the technique by traditional probes and consecutively we make a comparative analysis of the results with the ones obtained by the HTS-SQUID-based system. Within this type of approach novel tools to monitor niobium chemistry during fabrication of nuclear resonant cavities and to test current distributions inside current power modules used in motor for railway transportation both based on flux-gate magnetometry have been developed.

II. Experimental Systems

II.1 HTS-SQUID- based systems

A scheme of the eddy-current NDE system based on HTS-SQUIDs is shown in figure 1.

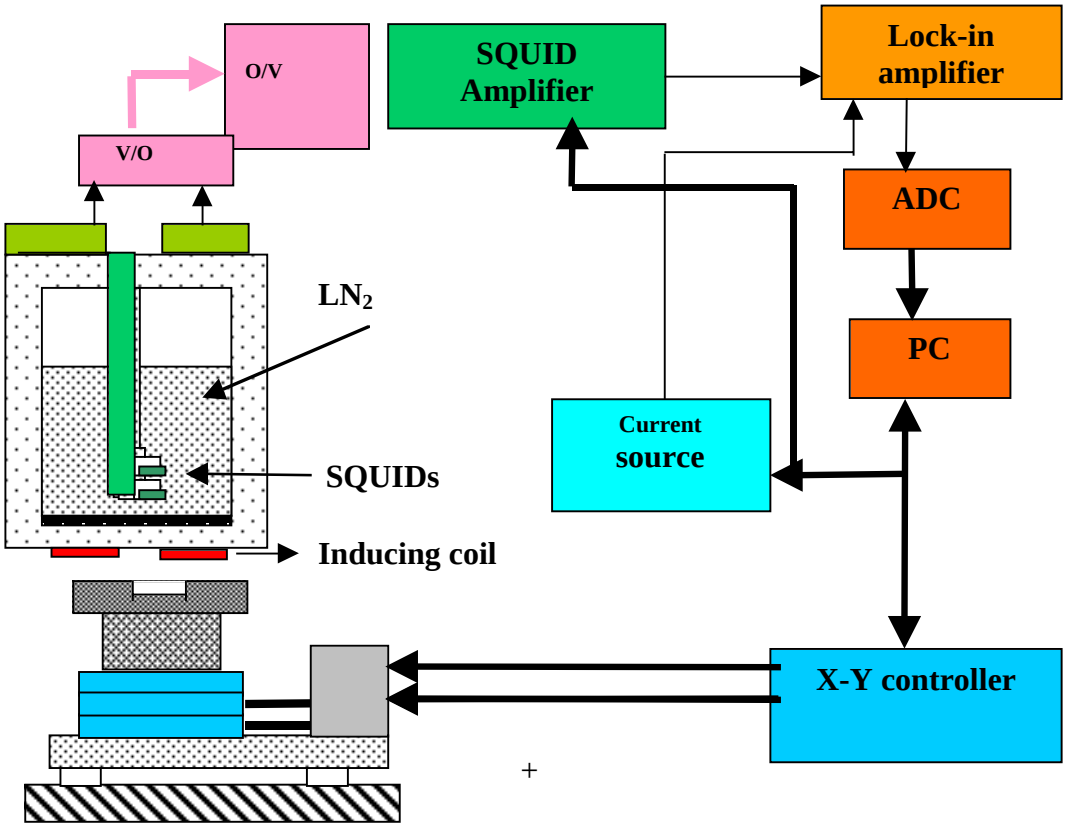

Fig.1*. A schematic of the eddy-current SQUID-based NDE prototype*

Depending on the specific application, the operating cryogenic temperature of 77 K is reached by liquid nitrogen-bath cooling using two different fiberglass cryostats. A 2-channels especially designed large one, has a measuring time of 7 hours at an evaporation rate of 0.7 l/h. The distance between the center of its bottom and the room temperature is less than 1 mm. The second one is a 1 liter and 3-channels cryostat which has a gap between the liquid nitrogen and the room temperature of about 5 mm. Pictures of the two systems are presented in figure 2 (a) and 2 (b), respectively.

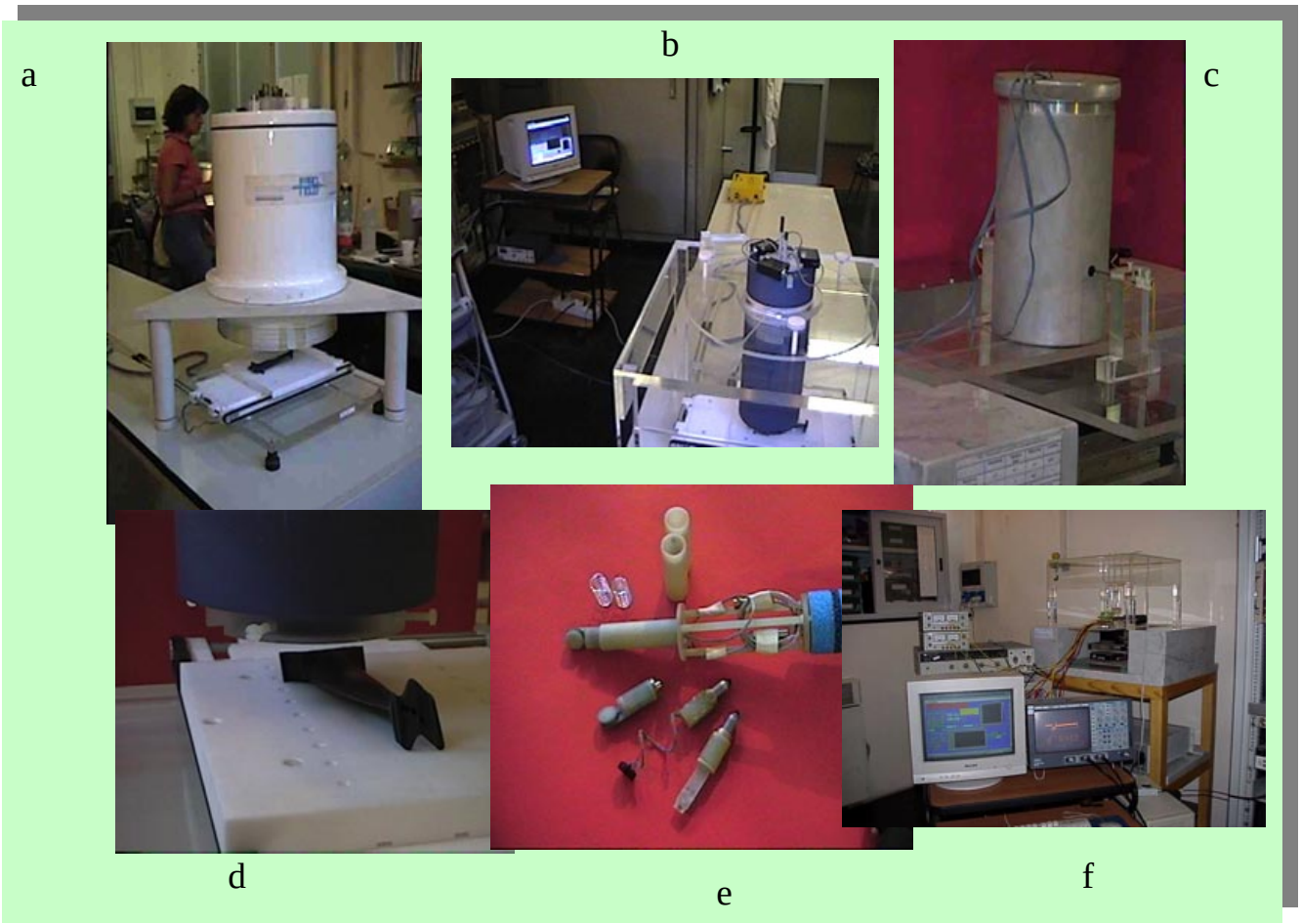

Fig. 2. Top figures: (a) *2-channels HTS SQUID-based NDE system;* ***(b)*** *3-channels HTS SQUID-based NDE system;* ***(c)*** *Fluxgate gradiometer in a e.m. shielded cilinder for the on-line test of superconductive wires;* ***Bottom figures****: **(d)** Detail of a aircraft turbine blade on a non metallic x-y positioning system below the 3-channels HTS-SQUID system****; (e****) Detail of the HTS SQUIDs used;* ***(f)*** *Experimental set-up for measuring the magnetic field by traditional e.m. probes (flux-gates and Hall probes) above power current modulus based on Insulated gate bipolar transistors.*

Eddy-currents are induced in the sample by a non-magnetic exciting source in order to avoid any electromagnetic coupling effects. In our configuration, the excitation coil is positioned beneath the stationary cryostat and it is parallel to the specimen. So far, we have mostly used a gradiometric double-D-shaped coil since in its center it presents a null value of the vertical *z* component and the horizontal *y* component of the magnetic flux density *B* existing above the sample. This differential arrangement ensures that, when measuring those components of the magnetic field, only distortions due to deviations of the eddy-currents inside the metallic structure by inhomogeneities like flaws are sensed. Thus, the ratio between the magnetic field induced on the surface of the sample and the one at the location of the SQUID in absence of flaws can reach the factor 10^4. In this way the dynamic range of the system (defined below) is increased.

The field penetration for this coil geometry is greater as compared to a planar spiral coil but the field profile is wider, thus reducing the spatial resolution of the system. Depending on the intended application, coils of diameters ranging between 5 mm and 60 mm have been employed. A coil with a larger diameter is required when deeply embedded defects are to be detected. In some cases, when measuring the component of the magnetic field parallel to the specimen we also used a 5 mm diameter circular exciting coil.

The systems use low noise HTS SQUIDs from Tristan, USA, from Forschungszentrum Jülich, Germany [Fig. 2 (e)] and from the Centro Nazionale Ricerche, Arco Felice, Naples, Italy. To mimic industry condition we operate in an electromagnetically unshielded environment with harsh magnetic conditions where the SQUIDs suffer from interference due to the main power (50Hz) and its harmonics (~200 nT) and to the earth's dc magnetic field (~50 μT). In order to reject noise disturbances from distant field sources, the outputs of two SQUIDs located at different distances from the sample may be electronically subtracted; thus, the first spatial derivative of the magnetic field is measured.

In this type of configuration (first-order electronic gradiometer), it is essential to optimize the distance between the SQUIDs (defined as baseline) to remove magnetic noise disturbances without

subtracting a significant amount of perturbed signal. The optimized baseline of 29.5 mm in the measurements on Al alloy samples shown in this paper, reduces to 20 nT the amplitude of the magnetic noise related to the main harmonic. The minimum distance between the bottom SQUID and the inducing coil (this being mostly constrained by the packaging of the probe) is 5 mm and 10 mm for the 3-channel and the 2-channel systems.

The alignment between the axial gradiometer and the center of the coil is achieved by moving the coil by a translation system that is placed just below the cryostat, as shown in figure 2 (d). The AC-source is a programmable low-noise HP3245A waveform synthesizer. A standard metallic two-dimensional scanning system or a fully non-metallic and nonmagnetic prototype with motors located 1.5 m away from the inspected sample, enable the sample to move beneath the stationary cryostat. Both data acquisition and X-Y positioning system are computer-controlled. The scanning range is 20 cm x 20 cm and the accuracy better than 15 μm and 100 μm respectively. Both of them enable to vary the scanning velocity to 50 mm/sec. In a typical measuring set-up, the sample is displaced at a speed of 1-5 mm/s, in a plane parallel to it, beneath the stationary coil and sensor. This yields to perform a single frequency line-scan or surface scan of the in-quadrature and in-phase components of the magnetic field (or its first order spatial derivative for a gradiometric configuration) which is expected to be characteristic of a defect in the sample. The SQUID output is analysed by an EG&G 5210 dual-channel lock-in amplifier, which demodulates and filters the output with a 6 Hz bandwidth.

To summarize a few of the essential parameters of the measurement system in unshielded environment (Tab.I), the magnetic field sensitivity of the system is less than 0.3 pT/√Hz rms for frequency above 100 Hz, the operating frequency ranges from 10 Hz to 26 kHz. The SQUID-read out system has a slew-rate of 10^3 and a dynamic range, defined as the ratio between the highest field change which can be measured before the electronics saturate and the lowest detectable field, of about 130 dB. This means we are able to detect magnetic fields due to small flaws in the presence

of large magnetic noise background produced, for example, by edge effect, or to simultaneously detect cracks at the surface and at the depth of more than 10 mm in highly conductive structures.

Magnetic field sensitivity SQUID magnetometer (shielded)	70 fT/ $Hz^{1/2}$
Magnetic field sensitivity first-order SQUID axial gradiometer (shielded)	100 fT/$Hz^{1/2}$, f > 100Hz
Magnetic field sensitivity first-order SQUID axial gradiometer (unshielded)	300 fT/$Hz^{1/2}$
3 dB Bandwidth	26 kHz
Dynamic range (shielded)	160 dB
Dynamic range (unshielded)	130 dB
Slew rate 1kHz	10^3 Φ_0/s
Maximum scan area	200 x 200 mm^2
Minimum step in x-y plane (metallic system)	15μm
Minimum step in x-y plane (non-metallic system)	100μm
Maximum speed	50 mm/s
Dewar bottom-room temperature distance 2-channel system	<1 mm
Dewar bottom-room temperature distance 3-channel system	~5 mm

Tab. I. *Main characteristics of HTS-SQUID based NDE system.*

II.2 Fluxgate-based system

A commercial low-noise three-axial flux-gate (Bartington), each in an 8x8x25 mm^3 package, has been used to compare the performance of different probes. The electronics of the flux-gate, operating at room temperature, is similar to the one described in figure 1 except for the voltage-optical converter that is not required. The unshielded magnetic field sensitivity is 30 pT/√Hz in the measurement range 10 Hz-1 kHz. The optimized baseline of the gradiometer is 30 mm for measurements on Al-alloy samples. The probe can be positioned at the minimum distances of a tenth of a mm from the specimen.

In Fig.2 (c) and 2 (f) a fluxgate gradiometer in a 5-layer e.m. shielded cylinder for the on-line test of room-temperature current-carrying Nb-Ti superconductive wires and the experimental set-up for measuring the magnetic field by traditional e.m. probes using a standard metallic x-y positioning system are shown, respectively.

II. 3 Induction coils

The induction coil test on Al-Ti alloy samples was performed using the absolute probe type *PKA 22-6* with a diameter of 38 mm and a thickness of 40 mm, at an operating frequency ranging from 50 Hz to 1 kHz. The maximum voltage sensitivity of this probe is 24 μV at 70 Hz. This particular kind of coil, optimized for operation at low frequency, has been chosen for a detection of deep flaws. It can be positioned on the surface of the specimen at a minimum distance of 0.3 mm.

The test on the damaged carbon fiber composite panels was performed using also an absolute probe PKA2-1 with a diameter of 1mm optimized to work in a frequency range 800 kHz-2.5 MHz.

II.4 Hall probe

The probe based on the Hall effect *Lohet II Honeywell,* used in this work has a magnetic field noise of 6 $\mu T/Hz^{1/2}$ at 1 Hz and a frequency bandwidth of 300 kHz. In figure 2 (f) the experimental set-up which uses also this kind of probe for measuring the magnetic field above power current modulus based on insulated gate bipolar transistors is shown. This traditional probe has a poor magnetic field sensitivity, but for its wide frequency bandwidth of operation, high spatial resolution and low cost has an interesting application when high current amplitude at a fast rate have to be detected.

III. Investigated Specimens

Some of the specimens analyzed in our work in the NDE field are shown in figure 3.
Most of them have been investigated within a collaboration research with Electrical, Chemical and Mechanical Departments of the University of Engineering of Naples, Italy or with other research centers and industries in Italy or abroad.

The 3 GHz copper resonant cavities and the two electrolytic Cu cells (fig. 3 top left) have been successfully used to monitor niobium chemistry during fabrication of nuclear resonant cavities by flux-gates.

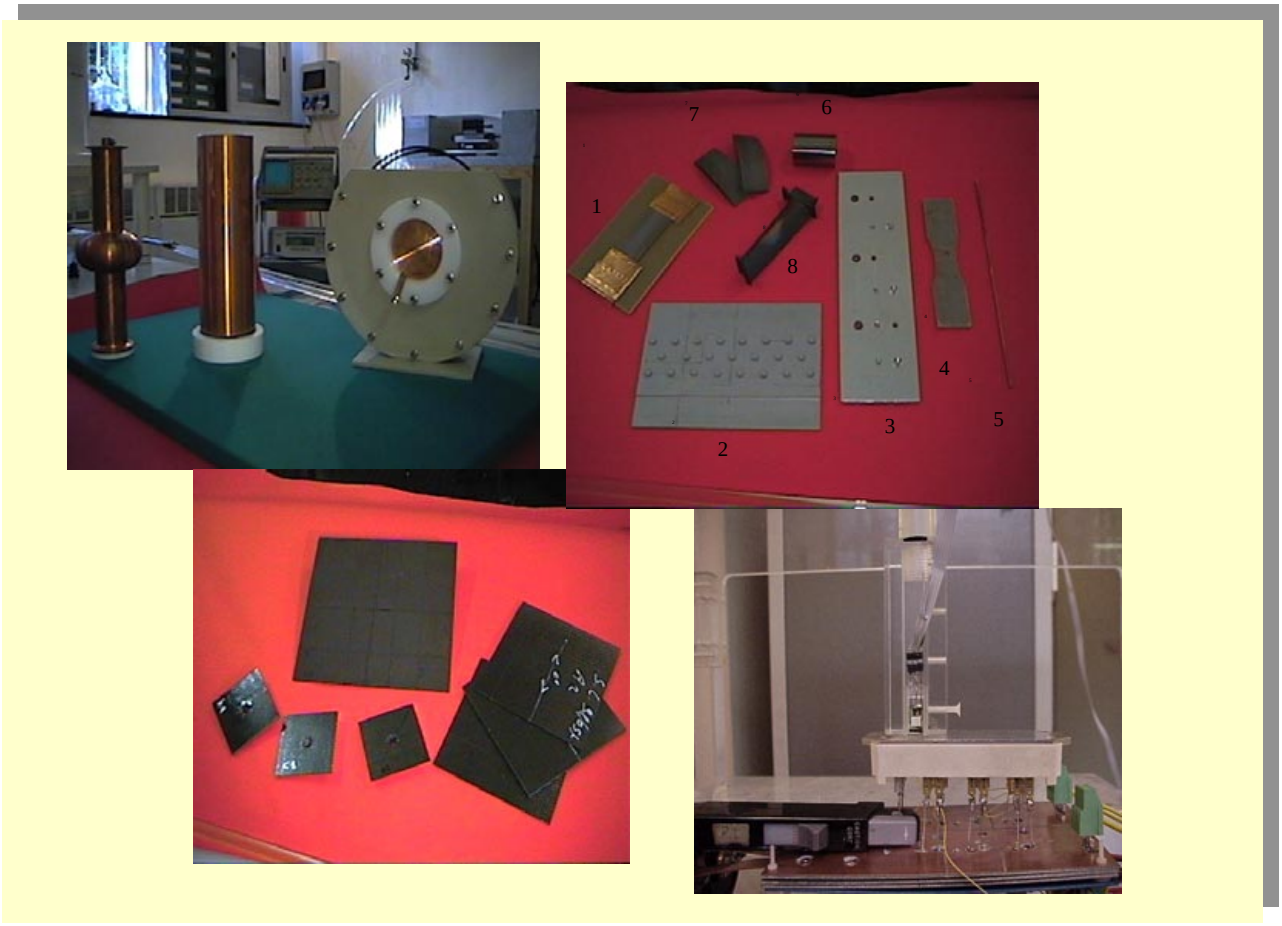

Fig. 3 Top figures: *Left: model of 3 GHz copper resonant cavities and two Cu electrolytic cells (V. Palmieri INFN-Padova, Italy); Right: Investigated metallic structures: steel foil* ***(1)*** *and steel bulk* ***(7)*** *(Di Iorio, Dept. of Mech. Eng. U. of Naples, Italy;* ***(2)*** *Aircraft Al-Ti multi-layered structures with rivet rows (H. Tretout, Dassault Aviation, France);* ***(3)*** *Multi-layered Al-Ti plates with different artificial holes;* ***(4)*** *Steel with internal stress due to fatigue cycle (Liguori, Dept. Mech. Ing. U. of Naples, Italy);* ***(5)*** *NbTi superconductive cable in a Cu matrix (R. Garre' Europa Metalli, Fornaci di Barga, Lucca., Italy);* ***(6)*** *steel cilinder with porousity defects (E. Vivo, FIAT-Avio, Naples, Italy);* ***(8)*** *aircraft turbine blade with embedded fatigue defects (E. Vivo,FIAT-Avio, Naples, Italy).*
Bottom figures: *Left: N-ply carbon fibe reinforced plates with damages due to different energy of the impact (D. Tescione, Cira, Capua, Italy; Caprino Chemical Eng. U. of Naples, Italy)*
*Right****:*** *Mitshubishi AC current power driver (with Insulated Gate Bipolar Transistors) used in railways transportation (G. Busatto, Dept. of Electrical Eng. U. of Cassino, Italy)*

Different small metallic specimen with real and artificial anomalies such as flaws, fatigue crack, inclusions, residual stress, porosity are shown in the top right of figure 3. Some of them, in addition to the ones shown in the next paragraph, have been investigated by induction coils, fluxgates and by HTS-SQUID based system.

The reinforced carbon-fiber polymer panels damaged by a drop weight machine at low-velocity impact (Fig. 3 left bottom) have been tested both by induction coils and HTS-SQUID based system.

To test current distributions inside power modules (Fig.3 bottom right), used in motor for railways transportation, both systems based on flux-gate and hall probe magnetometry have been developed.

These researches will be briefly summarized in this report.

IV. Superconductive and traditional probes for NDE of anomalies in metallic and composite structures

IV.I Detection of deep defects in Al-alloy samples

A typical gray-level area scan and a line-scan of the magnetic field normal to a Al-alloy sample affected by a surface-breaking flaw 20 mm long, 2 mm deep and 2 mm wide are shown in figure 4. By measuring the z-component of the eddy-current perturbation, we mainly detect effects from currents flowing in the x-y plane of the sample which are maximum at the outer edges of the slot. The electromagnetic interaction between the coil, which here has a differential geometry, and the flaw can be compared to that of a typical magnetic dipole.

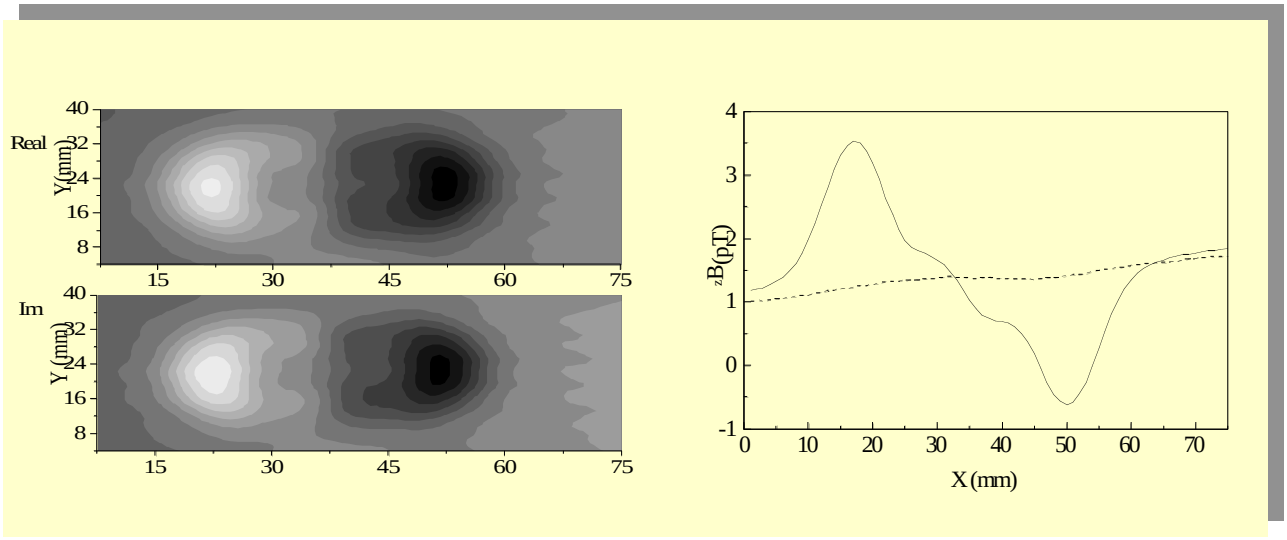

Fig.4 *Left: a gray-level area-scan of the in-phase (top) and the in-quadrature (bottom) part of the magnetic field component perpendicular to a surface-breaking, 20 mm long, 2 mm deep and 2 mm wide slot opening in air. The slot is cut at the center of a 3 mm-thick aluminum-alloy [7].*
Right: Line-scans retrieved from the map on the left for y=22 mm (above the mouth of the defect) and y= 40 mm (along an area far from the defect)[7].

However, the investigation of much smaller flaws or of deeply embedded defects in the conductivity structure requires an even higher sensitivity at low frequency.

For aircraft industry applications such as quality tests during the fabrication process or integrity assessments of structures already in use, it is essential to have a high accuracy in the localization of both surface and deeply embedded defects (depth >10 mm) in metallic structures. Since the skin penetration depth of the incident electromagnetic wave is given by $\delta = \sqrt{(\sigma_0 \mu_0 \pi f)}$ (where μ_0 is the magnetic permeability of vacuum, σ_0 the material conductivity and f the incident wave frequency), probes having a high sensitivity at low frequencies are required. In this context, a comparative study of nondestructive testing performed by traditional probes such as induction coil and flux-gate and the innovative one based on SQUID magnetometer is presented here. Five aluminum-alloy structures with artificial defects such as holes, slots and cracks, modeled after those commonly encountered in the aircraft industry, have been examined (Fig.5) [8].

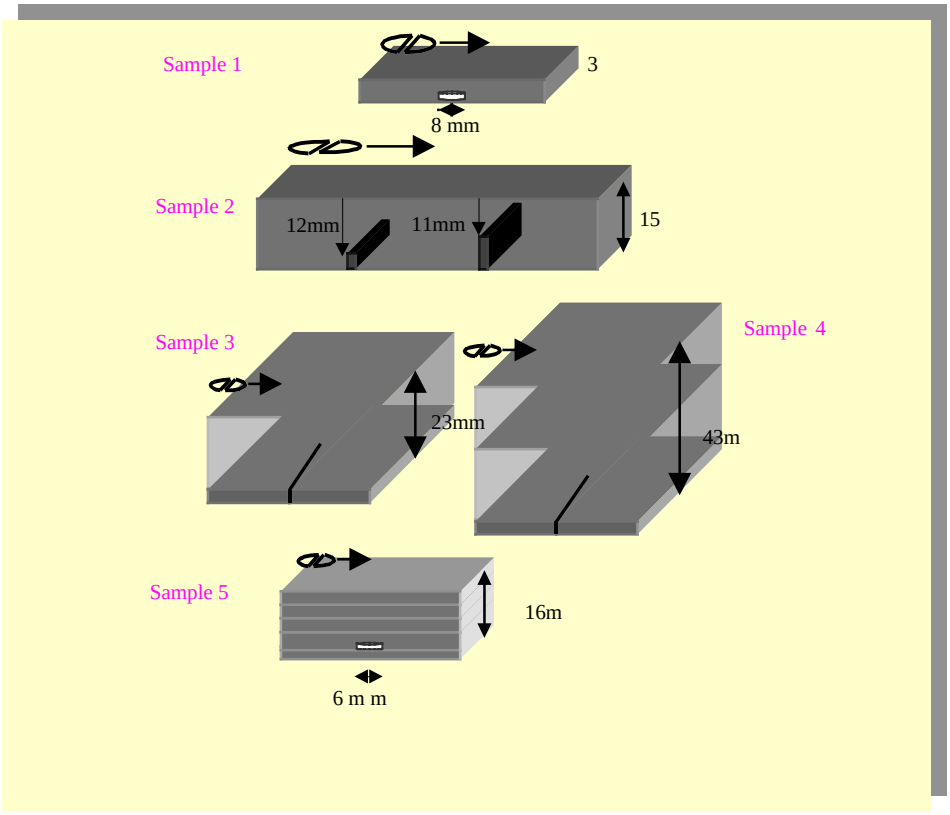

Fig. 5*. Sketch of the five aluminum-alloy structures with various defect configurations examined in this paper. Drawings are not to scale [8].*

In addition, the physical and geometrical characteristics of the samples are given in Tab. II. In the same table, the geometrical parameters of the defects affecting those structures as thickness (t), width (w), length (L), diameter (D) and depth (d) are also reported.

Test	Alloy	σ_0 (MS/m)	Overall Volume (mm^3)	Defect	t (mm)	w (mm)	L (mm)	D (mm)	d (mm)	Note
1	Al7071Ti651	32±20%	100x200x4	Circular hole	1			8	3	1-layer
2	Al7071Ti651	32±20%	150x1000x15	Multiple slots		0.6	40		12	1-layer
3	Anticorodal	56±20%	200x200x23	Crack	3	<0.1	400		20	2-layers
4	Anticorodal	56±20%	200x200x43	Crack	3	<0.1	400		40	3-layers
5	Al7071Ti651	32±20%	100x200x16	Circular hole	1			6	12	5-layers

Tab. II. *Physical and geometrical characteristics of the 5 aluminum-alloy samples which are shown in Fig. 3. σ_0, t, w, L, D, and d represent the electrical conductivity of the sample, and the thickness, width, length, diameter and depth of the particular defect, respectively [8].*

In eddy-current-NDE measurements, noise and signal depend on the particular defect to be detected and it is difficult to measure them separately. Moreover, due the intrinsically different working principle of the three probes, each is in effect measuring a different physical characteristic. Flux-gate, SQUID and induction coil detect the component of the magnetic field parallel with the core, the magnetic flux through the loop and the inductance variation, respectively.

The sensor-independent parameter chosen to perform such a comparison is a type of Signal-to-Noise ratio (S/N) defined as the ratio between the maximum signal variation along the measured line-scan (S_{pp}) and the standard deviation of the N data points b_i collected along the same line scan, i.e. $\sigma = [\sum_i (b_i - b_m)^2/N]^{1/2}$, where b_m is the average value of N points. Since in our measurements line-scans are crossing a consistent area of the sample located far away the defect, σ can be considered as a good approximation of the noise in each measurement.

In practice, due to the spatial extent of the sensors, the value and shape of the detected signal also depend on the tilt angle between the probe axis and the direction of the sample plane. This problem together with the effect of variation in the lift-off between sensor and sample has been carefully investigated for flux-gate and SQUID. For more details see ref [8].

To compare the probe sensitivity to deep flaws, output signals as a function of the line-scan coordinate were recorded for the samples. Each of the structures used in this study and described in figure 4 was chosen to test the sensitivity of the sensors in different circumstances. The simpler structure, sample 1, is affected by a sub-surface circular hole. Sample 2 gives information on the detection of multiple slots at depths greater than 10 mm in a single-layer structure. Measurements on samples 3 and 4 give information on the detection of a long crack in a three-layer structure at even larger depths (20 mm and 40 mm), which is severely testing the sensitivity of the probes, as shown below. Finally, sample 5 is used for the detection of a millimeter-sized defect in a 5-layer structure at depths larger than 10 mm. The presence of many layers and of insulating gaps between

them results both in a significant reduction of the conductivity of the whole structure and in complex wavefields reflected at the interfaces. The attenuation of the output signal can be significant in this case.

All the S/N data discussed are summarized in Tab. III. When it is no specified, a coil having a diameter of 25 mm is used as a source of eddy-current.

The induction coil and the fluxgate gave no measurable signal for samples 4 and 5, respectively.

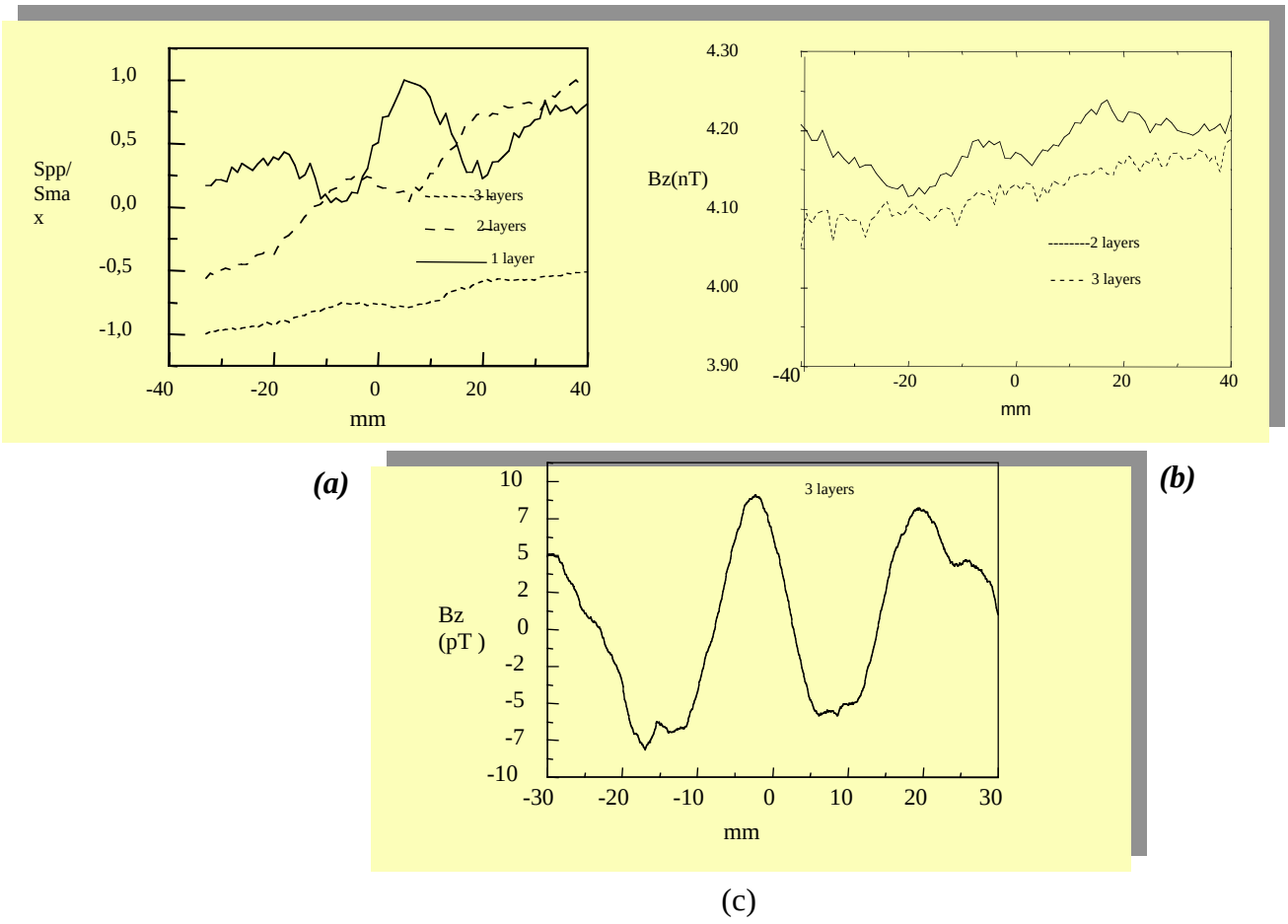

Fig. 6 (a): *Experimental results for the induction coil at 70 Hz above sample 5 (3-layers) and after removing one and two upper layers;* ***(b):*** *response of the flux-gate above sample 5 and after removing the upper layer at 133 Hz and 180 mA (b);* ***(c):*** *SQUID response at 120 mA above the sample 5 at 133 Hz [8].*

In particular we show in figure 6 the measurements on the last structure studied (sample 5, with insulating gaps between the stacked layers). The experimental results for the flux-gate with an exciting coil carrying a current of 180 mA at 133 Hz is shown in Fig. 6 (a). The output signal in this case did not reveal the defect even after lowering the frequency. After removing the upper layer, the probe detected a signal with a S/N = 1.85. The induction coil operating at 70 Hz detected the hole in sample 5 with a poor signal-to-noise ratio (S/N = 0.16). The response improved upon removal of one and two upper layers, as shown in Fig. 6 (b). Finally, Fig. 6 (c) shows the SQUID response with

a signal-to-noise ratio S/N = 3.57 for an inducing coil current of 120 mA at 133 Hz. In this challenging structure the superior performance of SQUID is clearly demonstrated.

Figure 7 summarizes the S/N ratios as function of defect depth for the above-described measurements. We emphasize finally that this study has compared the performance of intrinsically different probes in their optimized operating conditions. This has required optimization of the relevant parameters, for example, distance probe-coil and coil-sample, frequency and current, so as to maximize the S/N response for each probe rather than rigorously keeping the same values for all.

Sample	1	2	3	4	5
Coil S/N	2,58-1kHz 2.38-580 Hz 2.34 -70 Hz	0.65 -70Hz (11mm) 0.25 (12 mm)	0.92 70Hz	Non detected	0.164 70Hz
FG S/N	9.16 -1kHz 6.97-580Hz 2.84 -77Hz	2.46 -77Hz (11mm) 0.64 (12 mm)	3.59 133Hz* 2.07 133Hz	0.56 13Hz *	Non detected
SQUID S/N	2.621-1kHz 5.21-580Hz 2.19-77Hz	4.20 -77Hz (11mm) 1.95 (12 mm)	2.54 133Hz	2.78 13Hz *	3.573 133Hz

(*) exciting coil with a diameter of 58 mm

Tab.III. *Summary of the S/N ratios for the different probes in the examined samples [8].*

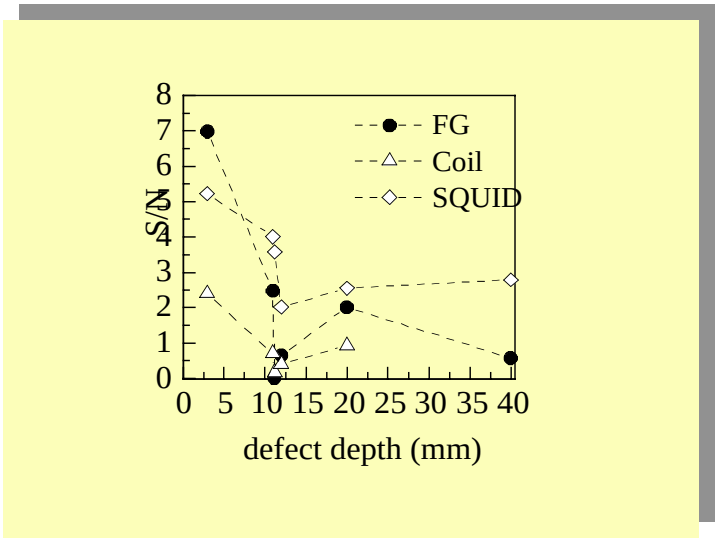

Fig.7. *Signal-to-noise ratio S/N versus the defects depth [8].*

IV.2. Reinforced carbon fiber polymer panels

Because of their high strength and stiffness to weight ratios, which facilitate high load-carrying capacity, carbon fiber reinforced polymer (CFRP) are widely used in aerospace applications such as panels in aircraft wings, tails and fuselage skins. However, due to the brittle epoxy matrix in which the carbon or graphite fibers are embedded, the laminates are susceptible to internal damage caused by impacts during their loading use. The damages can be induced by dropping a tool during maintenance, by hailstones, by bird strikes, by stone, by runway and so on. During an impact the fibers absorb part of the energy and distribute some of the load in an area as well as through the laminate thickness. This excess energy may lead to delamination, sub-surface matrix cracking, fiber/matrix debonding and fibres fracture, which in turn can cause reductions in static residual strength. An early and accurate detection of the extent of such impact damage is critical for keeping the integrity of both new and already in use structures.

Impact damage detection can be a difficult task, especially for low-velocity impacts when a signature of the damage has no visible surface manifestation. On the other hand, even such a tiny damages may affect the structural integrity of the material., since due to stress and strain their effects propagate during use altering the strength or stiffness of the component. For a common impact energy and impactor, a damaged specimen has a considerable strength loss in compression [9]. Thus, no matter how small they are, damages should be detected and accurately sized as soon as possible in order to facilitate monitoring of its growth.

Emerging technologies such as eddy-current testing by HTS-SQUID magnetometry could enhance both the detection and the characterisation of damages in composite materials due to its high sensitivity performances. Due to their high dynamic range the SQUIDs are able to detect magnetic fields due to small damages in the presence of large magnetic noise background produced, for example, by edge effect, or to simultaneously detect anomalies at the surface and inside the sample.

We carried on measurements of the magnetic field along a line-scan above damaged n-ply CFRP panels, by HTS-SQUID based eddy–current system, to detect any signature induced by low-velocity impact. The damages, artificially produced by an impact machine working in a stationary mode, are caused by impacts with an energy ranging between a few tenths of a joule to 40 Joule [10].

Measurements of the different spatial components of the induced magnetic field have been carried out in a wide frequency range. The performance of this innovative probe are demonstrated to be, in this particular investigation, superior to the ones of a commercial induction coil. In this summary we report on investigations performed on a 3 mm thick forth-ply carbon-fiber laminates with a stacking sequence [0/ 45°/90/-45°] artificially damaged by a 12 J impact (Fig. 8). For such a

impact, the damage is not visible on the hit surface but affects internally the sample and has the most effectiveness on the opposite surface. This makes the defect detection from the impacted surface, often the only accessible for investigation, a quite challenging task.

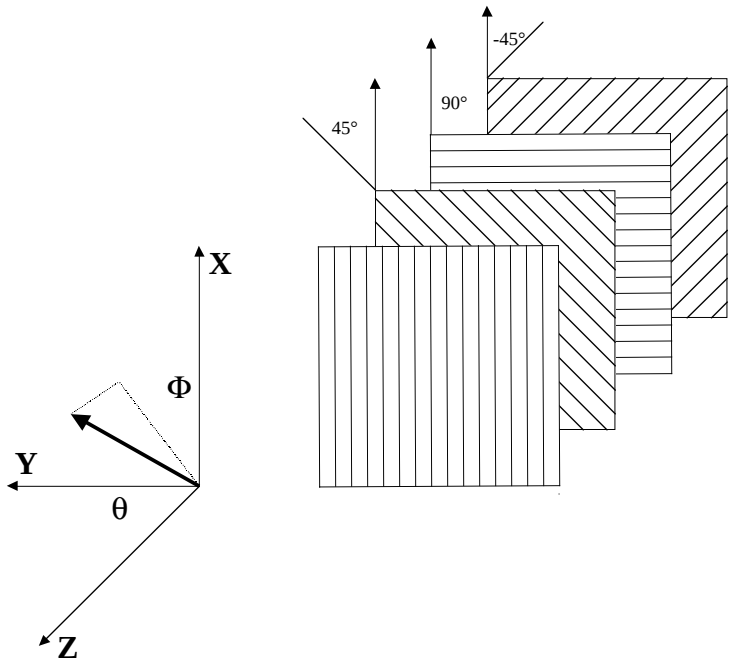

Fig. 8. *Sketch of the cross-ply carbon-fiber composite investigated. The stacking sequence [0/45°/90°/-45°] of the first 4 plies is shown. The angles α_i repeat every 4 plies. The carbon fibers in the ith-ply lie in the x-y plane and make an angle α_I with the x-axis.*

A comparison between the response of an HTS-SQUID based system and of an absolute induction coil operating at 2 MHz in detecting the damage from the impacted side and on the backside has been performed. Both probes enable to detect a signal with a good signal-to-noise-ratio from the damaged surface, but in the investigation from the opposite surface the induction coil fails while the SQUID succeeds in the detection. In figure 9 (a) and (b) line-scans of the three components of the magnetic fields along the x-axis measured by the HTS-SQUID above the impacted surface and above the back-side surface of the CFRP Panels are shown, respectively. The response of the induction coil along the x-axis and the y-axis, above the impacted surface is presented in figure 10.

The shape and the amplitude of the output signal of the two probes is mainly the results of the electrical and structural characteristics of the sample, the irregular shape of the defect and the geometry of the inducing and pick-up coil. The different attenuation factor in the amplitude of the three component of the magnetic field measured by the SQUIDs above the two opposite surfaces is related to the electrical anisotropy of the laminate.

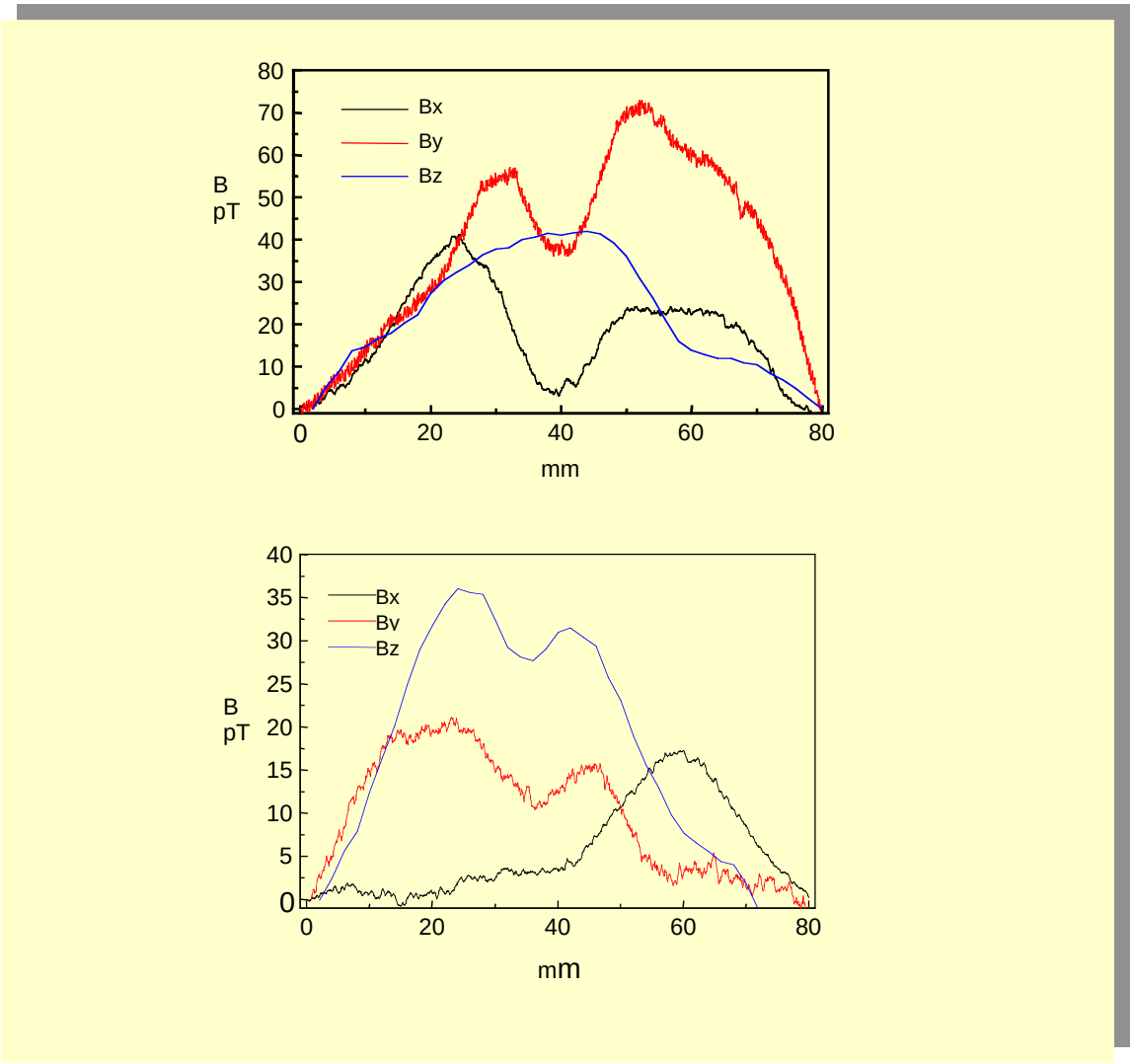

Fig. 9. *(a) Line-scans of the three components of the magnetic fields along the x-axis measured by the HTS-SQUID above the impacted surface (top) and above the backside (b) of the CFRP panel. The double-D shaped exciting coil carries a current of 180 mA at 10 kHz [unpublished].*

The failure of this particular type of coil does not exclude the possibility to succeed in the detection using a suitable one for this deep-lying defect. However, induction coils that operate at lower frequency to deepen the penetration depth of the e.m. wave, have a much lower spatial resolution and so, they are not optimized for the detection of surface and subsurface defects.

The energy threshold of the impact that results in a detectable damage by our system turns to be around 0.5 J for CFRP laminates with a thickness of 1mm [10].

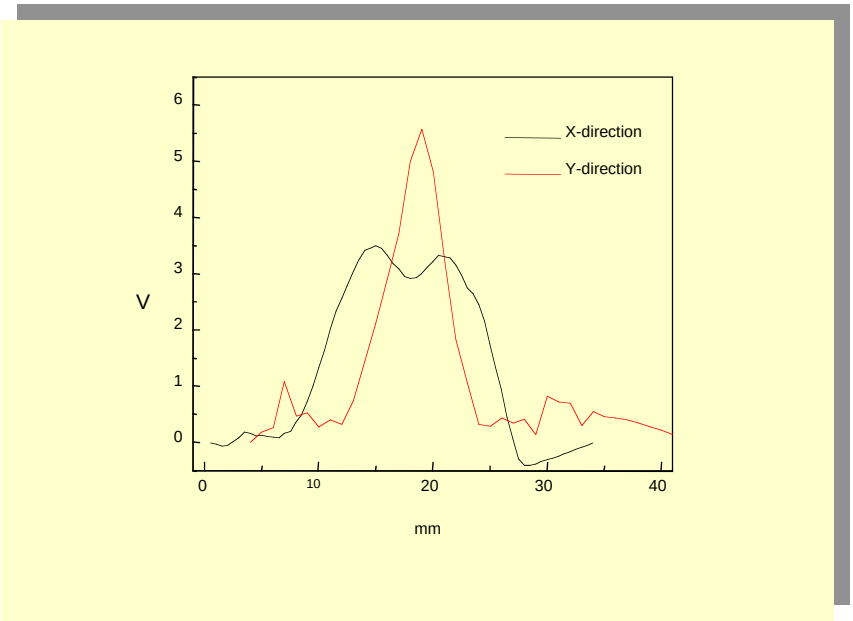

Fig.10. *Response of the absolute induction coil along the x-axis and the y-axis, above the impacted surface at 2 MHz[unpublished].*

V. Numerical simulations by VIM and FEM for planar metallic samples

For a better understanding of the electromagnetic phenomena which occurs in the detection of flaws in highly conductive structures and for an optimisation of the experimental set-up, a solution of the three-dimensional electromagnetic forward problem is necessary. It consists of modelling of eddy current and perturbed magnetic field generated by a defect with known electromagnetic characteristics, illuminated by a known source.

The simulations are carried out by a computational-fast vector volume integral method (VIM) dedicated to a planar layering affected by a volumetric defect, which is involving the elaborate construction of the Green's system of this layering, and additionally, by more general but slow Finite-Element methods (FEM).

The FEM code has been applied to our experimental geometry in which a gradiometric differential double-D shaped exciting coil and a SQUID gradiometer are displaced simultaneously in a plane parallel to the sample [11].

The high flexibility of this code provides the opportunity to tackle complex configurations in terms of both defect and sample geometry in order to investigate unknown currents and magnetic field distributions. Obviously, a high computational cost has to be paid in order to account for the simultaneous displacement of the SQUIDs and of the excitation coil. We find typically 80 hours

CPU time are required for computation of a few dozen discrete values of the vertical component of a single-frequency magnetic field above a millimeter-scale surface-breaking hole, carried out with a HP-UX workstation.

Comparison with a less computationally demanding formulation, even far less general, is certainly attractive. To that effect, a three-dimensional model based on a rigorous vector Volume Integral Method (the corresponding code is henceforth denoted as VIM), involving the elaborate derivation of the Green's system of the unperturbed structure, has been developed for the eddy-current nondestructive evaluation of non-magnetic planar isotropic structures affected by voids, cuts or inclusions [7 and 12]. A typical simulation now takes a few minutes CPU time for a hundred points relative to different SQUID-coil positions on a similar work-station, once a discrete counterpart of the Green's system is computed and stored.

In order to quantitatively compare synthetically-generated data and experimental data, we will always refer in the following to the line-scans measured above the mouth of the defect. As a first validation of our models, numerical simulation of the in-phase component of the line scan above a circular cylindrical defect in a plate is cross-checked with results obtained by the FEM code. Figure 11 shows excellent agreement between the two different models for a 2 mm deep surface-breaking circular cylindrical hole of 6 mm-diameter bored into a 4 mm-thick Al-Ti alloy plate [13].

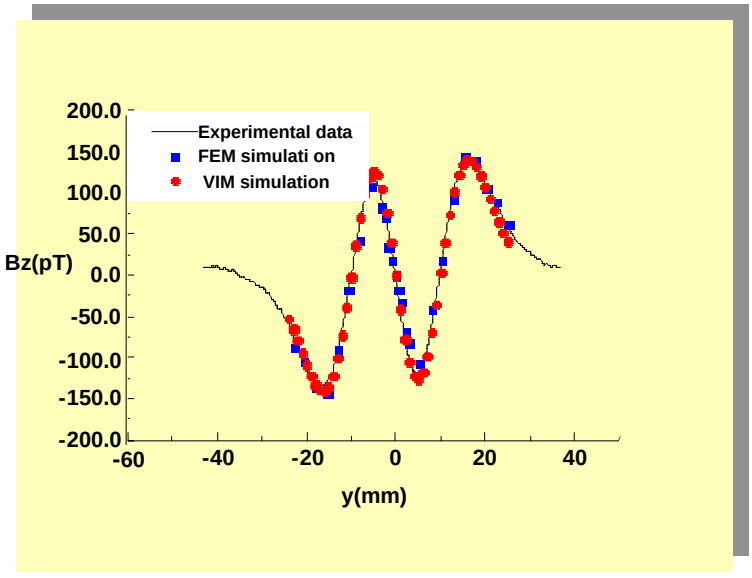

Fig.11. *Comparison between experimental data and numerical simulations performed by a Finite Element method (FEM) and a Volume Integral Method (VIM) for a surface breaking hole having a diameter of 6 mm and a depth of 2mm into an Al alloy plate. The 60-turns double–D shaped coil with a diameter of 25 mm carries a current of 1 mA at 1 kHz. In this case the distance between SQUID and coil and coil and sample are 12 mm and 11 mm respectively [13].*

Comparisons between experimental data and numerical simulations calculated by the much faster model based on VIM have been performed for different geometries of the flaws and for different component of the magnetic field above the sample.

A line-scan of the in-phase component of B_z above a surface-breaking 8 mm-diameter hole with a thickness of 2 mm is compared with the synthetic data in Fig. 12, top left [7]. The injected current amplitude in the 60-turn exciting coil is 1 mA and the working frequency is 1 kHz.

To take both the in-phase and the in-quadrature component of the magnetic field into account, in figure 12 (top right and bottom left) we compare the line-scans of the module of B_z obtained for 2 mm-thick rectangular slots in two different configurations. Measurements relative to a 4 mm x 2 mm slot embedded from the depth of 1 mm in the plate (top right) and to a surface-breaking 20 mm x 2 mm slot (bottom left) are compared with the numerical simulations [7]. In these last two measurements the 1-turn coil is fed by a current amplitude of 60 mA at a frequency of 1 kHz.

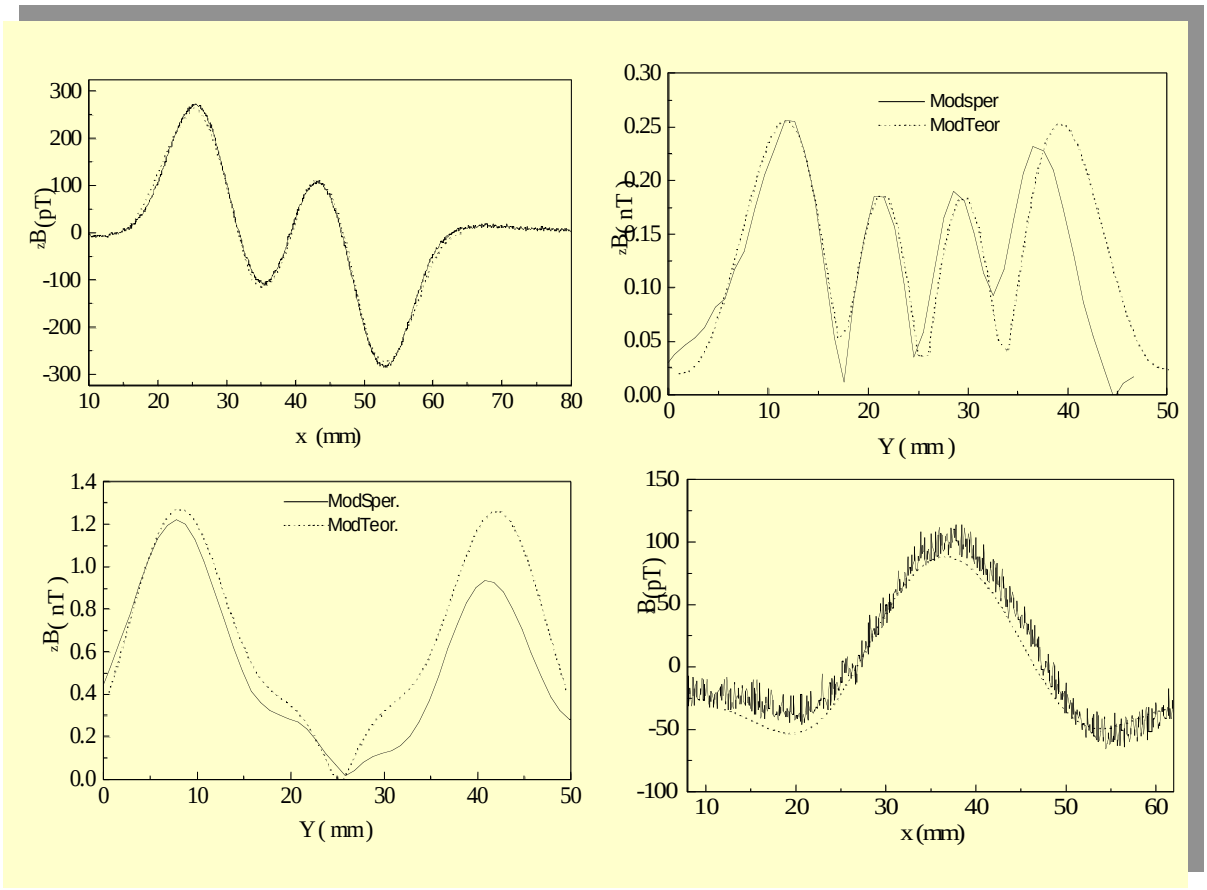

Fig.12. *Comparison between experimental data and numerical simulations performed by a Volume Integral Method (VIM).* ***Top left****: line-scan of the in-phase component of B_z above a 2 mm thick surface breaking hole having a diameter of 8 mm.* ***Top right and bottom left****: line-scans of the module of B_z obtained for 2 mm-thick rectangular slots in two different configurations. Measurements relative to a 4 mm x 2 mm slot embedded from the depth of 1 mm Al (top right) and a surface-breaking 20 mm x 2 mm slot (bottom left* ***Bottom right****: line-scan of the in-phase component of the magnetic field B_x as a function of the line-scan measured above a 20 mm-long, 2 mm-deep and 2 mm-wide rectangular slot embedded from a depth of 1 mm inside the plate is shown [7].*

To fully demonstrate the adequacy of the numerical modelling we still need to analyse measurements performed above defects lying inside the investigated structure and measurements of a component of the magnetic field different than B_z, as, for example, the one along the transverse *x*-axes to the sample.

In Fig. 12 (bottom right) the in-phase component of the magnetic field B_x as a function of the line-scan measured above a 20 mm-long, 2 mm-deep and 2 mm-wide rectangular slot embedded from a depth of 1 mm inside the plate is shown [7]. The single-turn exciting coil carries a current of 10 mA at 377 Hz.

The slight discrepancy occurring around the outer extreme in some comparisons may be related to a tilt of the sample or to a misalignment between the SQUID and the center of the double-D shaped exciting coil.

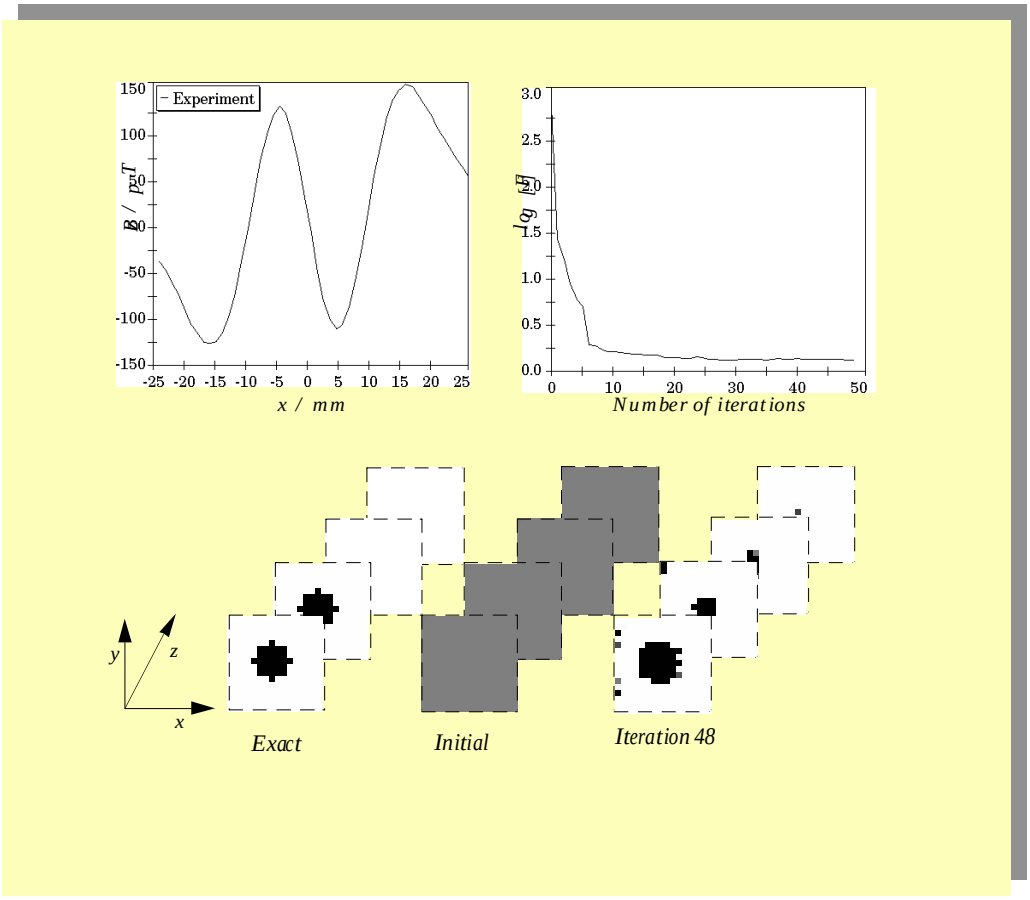

Fig. 13 *Reconstruction of a surface breaking 2 mm thick hole with a diameter of 6 mm cut in a Al-alloy slab after 48 iteration. The sketch represents the 4 mm thick Al plate as 4 layers of 1mm thickness each. [unpublished, courtesy of D. Lesselier and V. Monebhurrun].*

The excellent agreement when comparing synthetic results with experimental data in all cases, combined with a very low computational cost as compared to a finite-element technique, makes it a promising tool for solving the electromagnetic direct problem and to approach as a next step the

solution of the inverse problem in simple structures affected by a volumetric defect. Through the solution of this problem, maps of magnetic fields can be converted into images of the anomalies located into the material as shown in figure 13. Here we show the reconstruction of a surface-breaking 2 mm-thick hole with a diameter of 6 mm cut in an Al-alloy slab with a thickness. The Al slab in the computation is divided in 4 layers of 1 mm thickness each. After 48 iterations the approximate solution may be considered in a satisfying agreement with the exact solution, taking into account that it has been obtained from the single measurement along a line-scan of one component of the magnetic at one frequency.

Forthcoming experimental and numerical works will in particular aim at the inversion of two-dimensional maps of one or more components of multi-frequency time-harmonic magnetic fields as well as recording and possible inversion of pulsed eddy-current data. Our investigation will also be extended on samples with further complexity, e.g., more complicated defects like multiple defects or inclusions in multi-layered isotropic structures, and anisotropic layers (e.g. a N-ply carbon fiber composite) noticing that the numerical modelling of such anisotropic layers by a VIM-like method remains greatly challenging due to the shear complexity of the dyadic Green' s system and the uncertainties of the defects which may affect such layers.

VI. Novel Applications of Traditional Probes

VI.1. Magnetic field imaging of current distribution in IGBT power modules

Power semiconductor technology is developing toward new packaging techniques which enable to place several chips in parallel in order to obtain modules with the requested current handling capabilities. A not uniform current distribution among the chips can cause electrical, thermal and/or mechanical over-stresses inside the module, which in turns affects its reliability. The complexity of the internal layout of the power module makes its reliability assurance a very challenging task for nondestructive techniques. At present, the uniformity of the current distribution inside the device is indirectly evaluated by measuring the temperature underneath the chips. This measurement allows us to detect only the mean temperature of the chips during the switching. On the other hand a direct measure of the transistor collector current is particularly invasive and time consuming without a previous integration of the probe in the device at a manufactory level.

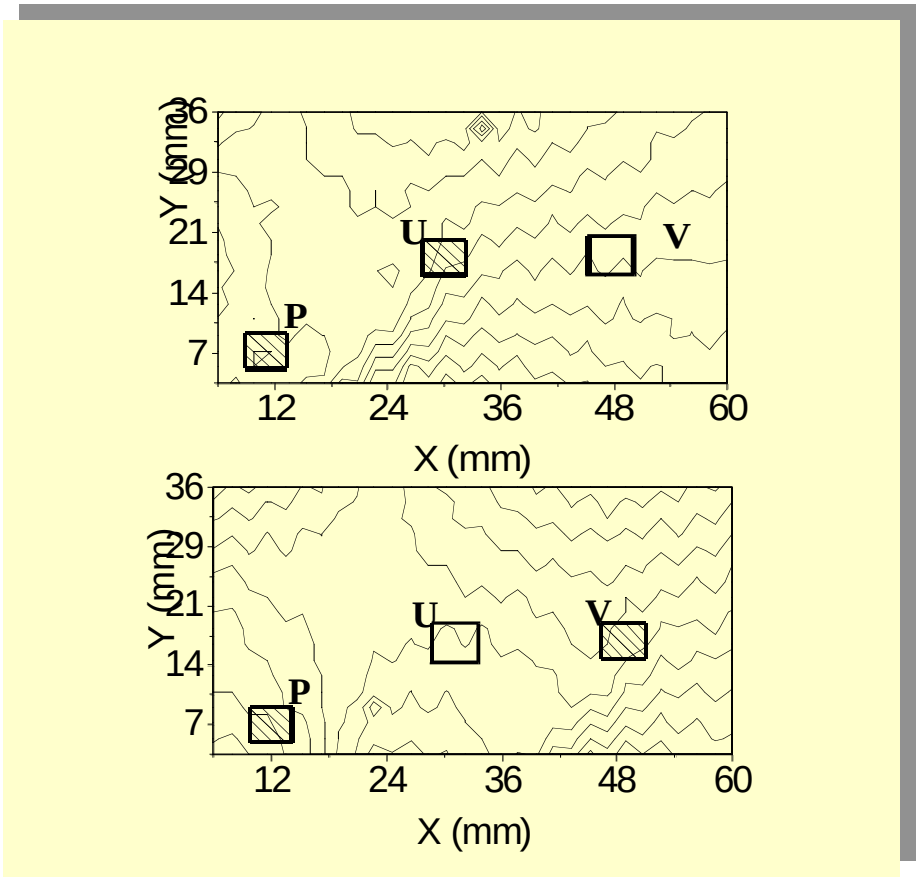

Fig.14 *Images of the magnetic field distributions above the device when the chips P-U (top) and the chips P-V (bottom) of the IGBT module are turned on. The amplitude of the magnetic field measured ranges between -24μT-21μT and –36 μT-26 μT, respectively [14].*

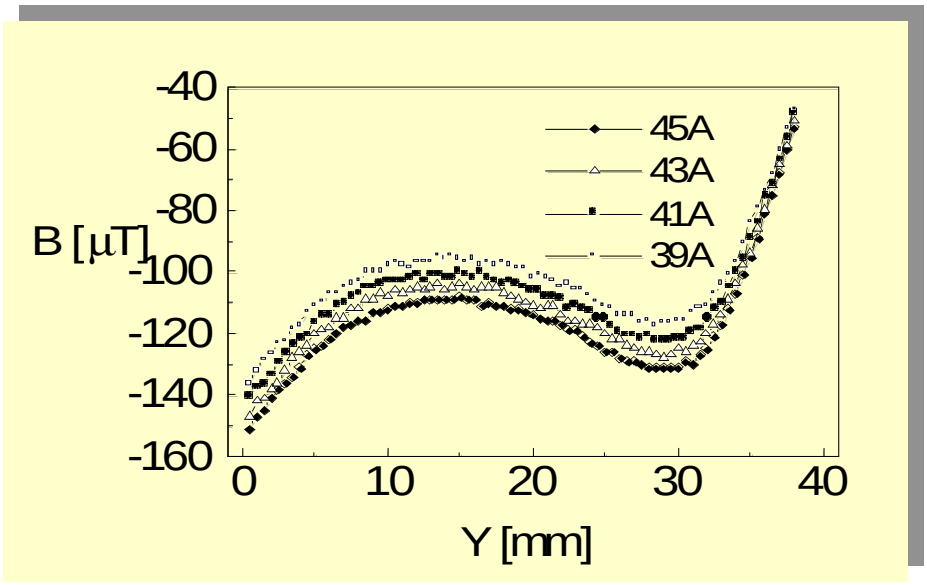

Fig.15*. Line-scans of the magnetic field as a function of the position above the transistors connected to the electrodes P-W and N-W driven by a current with an amplitude ranging between 39 A and 45 A [14].*

We present results obtained by a new tool of investigation of uneven currents inside an Insulated Gate Bipolar Transistor (IGBT) power module [14]. It consists on detecting the components of the magnetic field above the device by a magnetometer. Measurements have been performed by a probe based on the Hall effect on a power module made by six transistors, (Semitrans SKM 40 GD 123 D) driven by a pulsed current of high amplitude (40-50A). To independently control the chips in a switching regime a power current driver has been specifically developed for this investigation. Contour maps of the magnetic field components measured with different chips turned on each time, show clear signatures of changes both in the amplitude and path of the current distribution. To guarantee the correct working conditions of the many IGBT, inside the Safe Operating Area (SOA) of the device, the current sharing between the chips must be as uniform as possible to avoid an overloading of the transistors due to an excessive current. For this reason accurate measurements of the current unbalance between the single elements are essential to prevent failure of the module. The experimental results show the capability of this technique to measure unbalanced current between transistors with a resolution better then 5%.

The magnetic field distribution has been investigated when the chips connected to the electrodes labelled P, U and V were driven by a 45 A collector current for 200 μs and switched off for 100 ms. The 2-D maps above the device when the chips connected to the electrodes P-U and P-V are turned on, are shown in figure 14 (top and bottom). The amplitude of the magnetic field measured in the two cases ranges between –24 μT and 21 μT, –36 μT and 26 μT, respectively. The magnetic field distributions show a signature of the current concentration around the chips that are operating and along the bus-bars connecting the chips. From a database of magnetic images measured above the module when different chips are turned on, we are able to determine the location of the ones that are working with a position accuracy of 1 mm.

To test the current sensitivity of the system, i.e. to distinguish the unbalancing of the collector current driving two or more transistors, the magnetic field, was measured along a line-scan above the transistors connected to the electrodes P-W and N-W. In figure 15 the magnetic field around the maximum value of its amplitude measured along the line-scans, for currents ranging between 39 A and 45 A, are shown. The current sensitivity in this case is better than 5% as required by this application to avoid over stress of the transistors.

VI. 2. Monitoring of Niobium Chemistry during Fabrication of Nuclear Resonant Accelerator

Cavities

The buffered chemical polishing is almost a standard procedure applied in several laboratories in order to etch bulk Niobium/Copper resonant cavities for particle accelerators [15]. Even though the chemical polishing is only one of the many steps of the fabrication process, it is of a crucial importance for having a high quality resonator. Hence, although the process parameters are carefully monitored, frequently this polishing is just applied as a cookery recipe, and not as a result of an optimisation of the process parameters. In addition to that, the Niobium chemistry is a topic only marginally covered by literature so far.

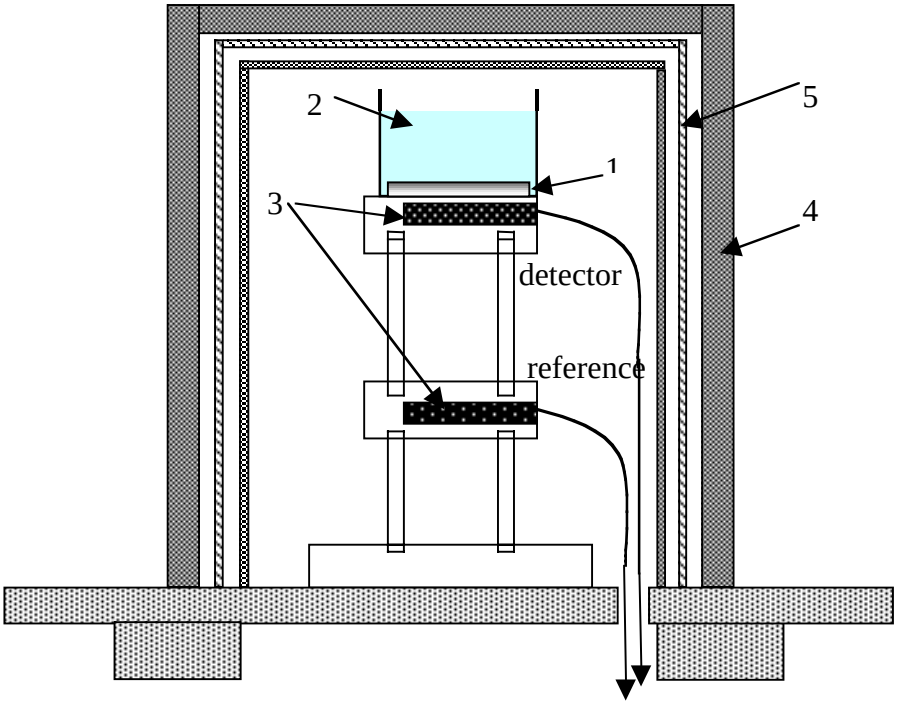

Fig. 16. *Experimental set-up for investigating the ongoing niobium corrosion. 1) niobium disk; 2) Teflon vessel filled with 40 ml of acid solution; 3) fluxgate magnetometers sensors housed in a plexi-glass holder. Detector and reference magnetometers are in a first order axial-gradiometric configuration; 4) aluminium shielding; 5) μ-metal shielding.*

Flux gate magnetometry has proposed as a novel diagnostic technique of the ongoing corrosion due to the buffered chemical polishing of Cu/Nb superconductive resonant cavities [16]. The detection of the magnetic field induced by the motion of the ions involved in the chemical process enables to detect the dynamics of the reaction from the area outside the resonator and, whenever the environmental magnetic noise is screened, it is very sensitive to the parameters of the process. In particular the preliminary results presented in ref. 16 confirm the possibility to investigate in a non-

intrusive and contact less method the corrosion of a copper cavities due to the chemical polishing and to correlate the Niobium etching rate to the measured magnetic field measured.

For a long time mixture of equal parts in volume of Hydrofluoric, Nitric and Phosphoric acid in the percentage 1:1:1 has been used. However, since H_3PO_4 is a moderator of the solution, more recently, a bath containing 2 parts of phosphoric acid (1:1:2) has been adopted. Indeed, even though the niobium etching rate decrease, there is the distinctive advantage to have a more controllable and thermally stable chemical reaction.

In order to detect a correlation with the etching rate of Niobium, the c omponent of the magnetic field parallel to the disk has been monitored during 18 min of chemical etching, in a frequency bandwidth 0-1.5 Hz, as a function of different percentage (x between 1 and 2) of H_3PO_4 in the 1:1:x solution (Fig. 16). The linear behavior of the magnetic field spectrum integrated in the bandwidth as a function of the phosphoric acid percentage (Fig. 17, left) remarks the linearity of the device for this application. Other measurements of disk weight enable to correlate the average of the magnetic field to the Niobium etching rate (Fig. 17 right).

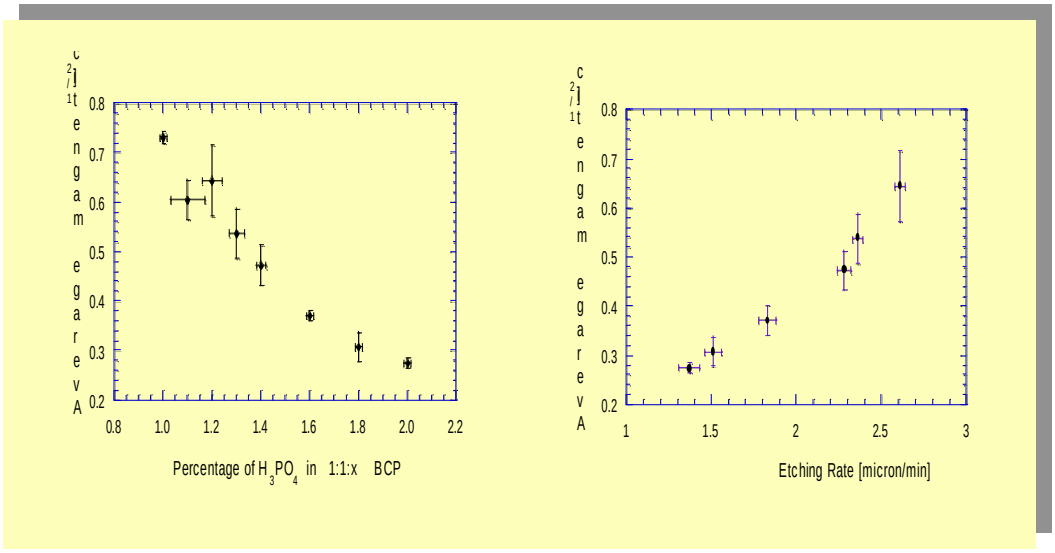

Fig. 17. *Component of the magnetic field parallel to the niobium disk during chemical etching, integrated in a frequency bandwidth 0-1.5 Hz as a function of the H_3PO_4 percentage (left) and of the etching rate (right) [16].*

Monitoring of the magnetic signal above a model of a 3 GHz resonant copper cavity across which a flow of ammonium Persulphate was fluxed has also been performed (Fig. 18). The difference in the corrosion effect at the equator and at the cut-off tube close to the iris has been investigated [16].

Moreover the same diagnostic technique is proposed to monitor the electro-polishing process of

the copper cavities used as substrate for the successive step of Niobium sputtering. The technique is contact less, nonintrusive and enables the measurements of the magnetic field in the range of pico-Tesla.

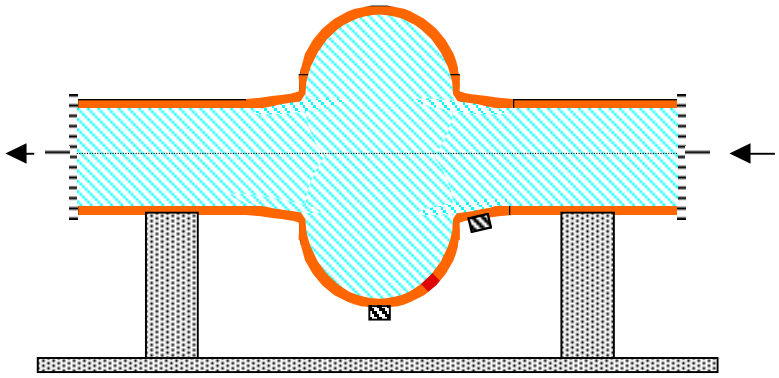

Fig. 18. *Monitoring of the corrosion process of a 3 GHz resonant cavity across which a flow of Ammonium Persulphate is fluxed. Two flux-gates detect the magnetic field at the equator and at the cut-off tube close to the iris [16].*

VII. Conclusions

A quantitative comparison between performance of different eddy-current probes has been carried out on materials used in aerospace applications, such as Al-alloy and carbon fibers, affected by defects. In particular, the performance of an induction coil, a flux-gate and a HTS-SQUID-based magnetometer has been investigated on the basis of comparative experiments on five Al-alloy test samples with artificial defects such as holes, slots and cracks and on cross-ply reinforced carbon fibers polymer panels damaged by low-velocity impacts. The overall superiority of the SQUID sensor performance is demonstrated in these particular niches of applications. While it always equally or more sensitive than the other sensors in each individual case, it is the only sensor which succeeds in identifying the defects in all the structures examined here.

To evaluate the accuracy and reliability of the measuring system two three-dimensional numerical models of the eddy-current perturbation (direct electromagnetic problem) have been developed for highly conductive and homogenous planar structure. One of them is based on the finite element method (FEM) and the other is cast in a vector wave-field integral equation framework (VIM). Both numerical solutions correctly predicts the shape and amplitude of the complicated magnetic field response which results from the shape of the defects, the geometry of the inducing coil and the characteristics of the SQUID gradiometer. The excellent agreement with

experimental measurements, combined with a very low computational cost as compared to a finite-element technique, led to successfully use the VIM as tool for solving the electromagnetic direct problem and retrieving the geometrical parameter of the defects.

In the framework of the non-destructive evaluation, we also demonstrated the feasibility of new investigation techniques in emerging fields of application of the magnetometry, by room-temperature probes. Novel tools to test current distributions inside current power modules used in motors for railway transportation and to monitor niobium chemistry during fabrication of nuclear resonant cavities, based on flux-gates and Hall probes have been developed.

The research on the magnetic field distributions in modules based on insulated gate bipolar transistors, fulfilled the requirement of this application, i.e. to measure, non-destructively, unbalanced current distribution among the chips within 5% of their driving current. Such a current variation, indeed, may cause electrical, thermal and/or mechanical over-stresses inside the module affecting, in turns, its reliability.

Measurements of the magnetic field induced by the motion of the ions involved in the chemical etching of Niobium, confirm the possibility to investigate, in a non-intrusive and contact less method, the ongoing corrosion of Niobium during the chemical polishing of Niobium/Copper accelerator cavities and to correlate the Niobium etching rate to the measured magnetic field.

Acknowledgements

We are grateful to G. Peluso co-ordinator of the INFM project and to G. Pepe which collaborated in the research presented here. D. Lesselier,V. Monebhurrun, B. Duchêne of DRÉ-LSS, CNRS-SUPÉLEC, Gif-sur-Yvette Cedex, France and D. Tescione of Centro Ricerche Aerospaziali, Capua, Italy are greatly acknowledged for their work on the numerical simulations based on VIM and FEM, respectively. Many thanks also to M. Prencipe for useful suggestions on eddy-current NDE carried on by traditional probes and to V. Palmieri and G. Busatto for their collaboration in the applications of the novel applications in Electrical Engineering, and Nuclear Physics.

We would like also to thanks A. Barone, H. Weinstock, J. Wikswo, A. Braginski, W. Podney, G. Donaldson, P. Seidel, D. Lesselier, V. Monebhurrun, M. Falay, H. Krause R. Fagalay, C. Carr, R. Albanese, G. Rubinacci, G. Romani, E. Sarnelli, S. Pagano and G. Testa for their many suggestions and incouraging during these years.

We dedicate this summary of our NDE work to S. Di Chiara.

This work has been carried out in the frame of the following projects: *Eddy Current Non-destructive Evaluation Using Superconducting Devices* with the support of the National Institute for Matter Physics (INFM) co-ordinated by Prof. G. Peluso; *Scanning high-Tc SQUID System*, funded by the European Community through INTAS 97-0894, co-ordinated by Prof. P. Seidel; and within the international collaboration contract *Nondestructive evaluation based on HTS-SQUID* between INFM, Italy and DRÉ-LSS, CNRS-SUPÉLEC, France.

This publication is based on the presentation made by A. Ruosi at the European Research Conference (EURESCO) on the "Future Perspectives of Superconducting Josephson Device: Euroconference on Physics and Application of Multi-Junction Superconducting Josephson Devices, Acquafredda di Maratea, Italy, 1-6 July 2000, organised by the European Science Foundation and supported by the European Commission, Research DG, Human Potential Programme, High-Level Scientific Conferences, Contract HPCFCT-1999-00135. This information is the sole responsibility of the authors and does not reflect the ESF or Community's opinion. The ESF and the Community are not responsible for any use that might be made of data appearing in this pubblication.

References

[1] *Non destructive evaluation of metallic structures using a SQUID gradiometer*, H. Weinstock and M. Nisenoff, in H.D.Halbohm and H.Lubbig (eds), SQUID'85, de Gruyter, (1985).
[2] *SQUID magnetometers for biomagnetism and non-destructive testing: important questions and initial answer*, J.P. Wikswo, IEEE Trans. Appl. Superconductivity 5, 74-120
[3] Cochran, G.B. Donaldson, L.N.C. Morgan, R.M. Bowman, K.J. Kirk, in Brit. J. NDT 35, pp.173-182
[4] *Electronic axial gradiometers for unshielded environment operating at 77K*, J. Borgmann, H. J. Krause, G. Ockenfub, J. Schubert, A. I. Braginski, P. David, presentd at EUCAS 1997
[5] High-transition-temperature superconducting quantum interference devices, D. Koelle, R. Kleiner, F. Ludwig, E. Dantsker and J. Clarke, Reviews of Moder Physics, 71, 3 (1999)
[6] *A new project on nondestructive evaluation with high temperature SQUID's*, Peluso, G. Pepe, A. Ruosi, A. Barone, P. Buonadonna, R. Teti, M. Valentino, U. Klein, C. Attanasio, L. Maritato, M. Salvato, C. Camerlingo,S. Pagano, M. Russo, E. Sarnelli, M.Prencipe, Review of progress in QNDE Vol. 16, eds. D. O. Thompson and D. E. Chimenti, Plenum, New York, (1997).
[7] *High Tc SQUIDs and Eddy-current NDE: a Comprhensive Investigation from Real Data to modelling*, A. Ruosi, M. Valentino, G, Pepe, V. Monebhurrun, D. Lesselier, B. Duchêne, to be published on Meas. Sci. Technol. (2000)
[8] *Superconductive and electromagnetic probes in eddy-current NDE for detection of deep defect*, M. Valentino A. Ruosi, G. Pepe, V. Monebhurrun, D. Lesselier, Studies in Applied Electromagnetics and Mechanics, 15, D. Lesselier and A. Razek (eds), IOS Press Amsterdam (1999)
[9] *An Experimental Study of Low Velocity Impact Damage in Woven Fiber Composites,* Y.P.Siow and V.P.Shim, , J. of Composite Mat., 32 (1998) pp. 1178-1202
[10] *Analysis of low-velocity impact damages in reinforced carbon fiber composites by HTS-SQUID magnetometers*, A. Ruosi, M. Valentino, G. Pepe, G. Peluso, IEEE Trans. Appl. Superconductivity (2001), to be submitted on sept. 2000
[11] *Electromagnetic SQUID based NDE: a comparison between experimental data and numerical FEM modelling,* G. Pepe, G. Peluso, A. Ruosi, M. Valentino, D. Tescione, Review of progress in QNDE Vol. 17, eds. D. O. Thompson and D. E. Chimenti, Plenum, New York (1998)
[12] *Eddy-current nondestructive evaluation using SQUIDs: the forward problem*, V. Monebhurrun, D. Lesselier, A. Ruosi, M. Valentino, G. Pepe, Studies in Applied Electromagnetics and Mechanics, 15, D. Lesselier and A. Razek (eds), IOS Press Amsterdam (1999)
[13] *Experimental and Theoretical results in e.m. nodestructive testing with HTS SQUID,* A. Ruosi, M. Valentino G. Pepe, G. Peluso, " IEEE Trans. Appl. Superconductivity, 9 (1999)
[14] *Magnetic Field Imaging of Current Distributions in IGBT power Modules*, M. Valentino, A. Ruosi, G. Pepe, G. Busatto, submitted to Studies in Applied Electromagnetics and Mechanics, 16, IOS Press Amsterdam (2000)
[15] *A selection of higher gradient cavity experiments* , P. Kneisel, Proceedings of the 8 th workshop on RF superconductivity, Abano Terme, V. Palmieri, A Lombardi (eds.), LNL-INFN (Rep) 133/98, (1997)
[16] *Fluxgate Magnetometry: The possibility to Apply a Novel Tool to Monitor Niobium Chemistry*, V. Palmieri, F. Stivanello, M. Valentino, Proceedings of the 9th Workshop on rf Superconductivity, Santa Fe', New Mexico, USA (1999)